

Yoshimi Sueishi*, Keitaro Miyazono, and Kazuki Kozai

Effects of Substituent and External Pressure on Spin Trapping Rates of Carbon Dioxide Anion, Sulfur Trioxide Anion, Hydroxyl, and Ethyl Radicals with Various PBN- and DMPO-Type Spin Traps

Abstract: Using a competitive trapping method employing two different traps, the trapping rates of anionic radicals ($\text{CO}_2^- \cdot$ and $\text{SO}_3^- \cdot$), hydroxyl, and ethyl were quantified for various PBN- and DMPO-type traps. We have examined the characteristic effects of substituent and external pressure on the spin trapping of anionic radicals and compared with those of neutral radicals such as ethyl and hydroxyl radicals. In DMPO-type traps, the effects of substituent on trapping rates of two anionic radicals were small compared with that of $\text{C}_2\text{H}_5\cdot$. In PBN-type traps, the large effects of substituent on trapping rates of $\text{CO}_2^- \cdot$ and $\text{C}_2\text{H}_5\cdot$ were observed. Further, the activation volumes determined from the pressure dependence experiments for competitive reactions show a difference in pressure behavior between the two trapping reactions, and enable us to speculate on the reaction mechanism of substituted PBN and DMPO traps for anionic radicals.

Keywords: High-Pressure ESR, Spin Trap, Substituent Effect, Trapping Rate.

DOI 10.1515/zpch-2014-0538

Received May 14, 2014; accepted July 20, 2014

1 Introduction

Spin trapping involves the trapping of reactive free radicals by an addition reaction to produce more stable radicals, detectable by electron spin resonance (ESR) spectroscopy, and has become a valuable tool in the study of transient free rad-

*Corresponding author: Yoshimi Sueishi, Department of Chemistry, Faculty of Science, Okayama University, 3-1-1 Tsushima Naka, Kita-ku, Okayama 700-8530, Japan,
e-mail: ysueishi@cc.okayama-u.ac.jp

Keitaro Miyazono, Kazuki Kozai: Department of Chemistry, Faculty of Science, Okayama University, 3-1-1 Tsushima Naka, Kita-ku, Okayama 700-8530, Japan

icals in chemical and biological systems [1–3]. Nitron compounds such as 5,5-dimethyl-pyrroline-1-oxide (DMPO) and α -phenyl-*N*-*tert*-butylnitron (PBN) have been most widely used as spin trapping compounds. It is recognized that nitron traps form stable radical adducts with neutral radicals such as hydroxyl and alkyl radicals. However, the basic information for the trapping rates of various nitron traps against ionic radicals has not been well established because of the short-lived ionic radical adducts.

Various sulfites are used as sanitizing agents in the food industry and are recognized as safe. However, the sulfur-center trioxide anion radical ($\text{SO}_3^{\cdot-}$), which is formed during sulfite metabolism via one-electron oxidation, is proposed as contributing to the mechanisms of toxicity [4]. Therefore, it is important to collect basic data regarding the spin trapping of various nitron traps against anionic $\text{SO}_3^{\cdot-}$ radical.

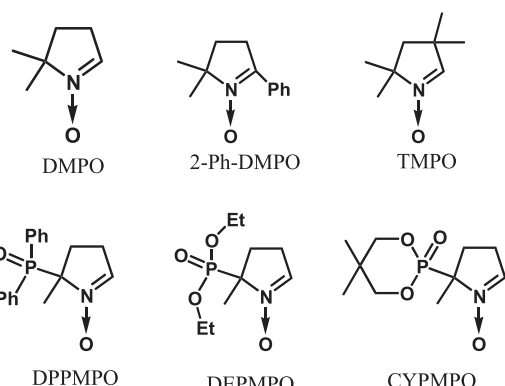
In this study, since the $\text{SO}_3^{\cdot-}$ and carbon dioxide anion ($\text{CO}_2^{\cdot-}$) radicals form relatively stable spin adducts with nitron traps [5, 6], we have determined the anionic $\text{SO}_3^{\cdot-}$ and $\text{CO}_2^{\cdot-}$ radical spin trapping rates for various PBN- and DMPO-type traps, using a competitive trapping method. We then compared those rates with the spin trapping rates for neutral radicals such as hydroxyl and ethyl radicals. Further, we investigated the effects of substituent and external pressure on the spin trapping rates for various PBN- and DMPO-type traps. Examination of the pressure effect on chemical reactions is useful in characterizing the reaction mechanism. Based on the experimental results, we have performed substituent and volumetric studies on the spin trapping reactions.

2 Experimental

2.1 Material

The spin traps illustrated in Figure 1 were used in the present study: 5,5-dimethyl pyrroline-1-oxide (DMPO), 2,2-dimethyl-5-phenyl-3,4-dihydro-2*H*-pyrrole 1-oxide (2-Ph-DMPO), 2,2,4,4-tetramethyl-3,4-dihydro-2*H*-pyrrole 1-oxide (TMPO), 5-di-phenylphosphoryl-5-methyl-3,4-dihydro-2*H*-pyrrole 1-oxide (DPPMPO), 2-(diethoxyphosphoryl)-2-methyl-3,4-dihydro-2*H*-pyrrole 1-oxide (DEPMPO), 5-(2,2-dimethyl-1,3-propoxyl cyclophosphoryl)-5-methyl-1-pyrroline *N*-oxide (CYPMPO), benzylidene(*tert*-butyl)amine *N*-oxide (α -phenyl-*N*-*tert*-butylnitron (PBN)), *tert*-butyl(4-pyridinylmethylene)amine *N*-oxide (4-POBN), *tert*-butyl(4-hydroxybenzylidene)amine *N*-oxide (4-HO-PBN), *tert*-butyl(2-sulfonatobenzylidene)amine *N*-oxide (2-SO₃⁻-PBN), *tert*-butyl(4-nitorobenzylidene)amine *N*-oxide

DMPO-type spin traps



PBN-type spin traps

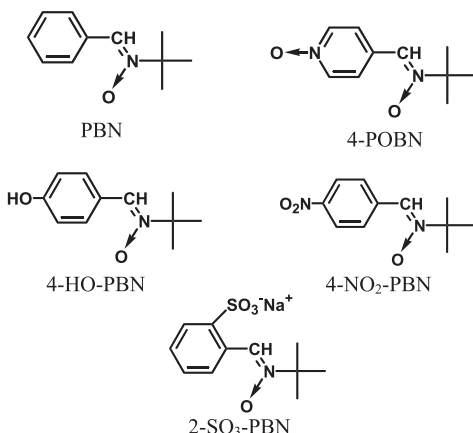


Figure 1: Structures of DMPO- and PBN-type spin traps.

(4-NO₂-PBN). DEPMPO and CYPMPO were purchased from Radical Research Inc. (Hino, Japan). 4-OH-PBN and 2-Ph-DMPO were synthesized at the OMRF Laboratory (Oklahoma City, OK, USA). Other PBN- and DMPO-type traps were obtained from Aldrich Chemical Company, Inc. (Milwaukee, WI, USA) and Wako Pure Chemicals (Osaka, Japan). Spin traps were used as received. Sodium sulfite and sodium formate (+ hydrogen peroxide) were used as a source of sulfite anion trioxide radical (SO₃^{·-}) and carbon dioxide anion radical (CO₂^{·-}), respectively [5–7]. The solvent used was distilled water.

2.2 ESR measurements

The CO_2^\cdot radical was generated with UV irradiation of the phosphate buffer ($\text{pH} = 7.4$) containing NaHCO_2 (100 mM) and H_2O_2 (100 μM) [7]: 5 s irradiation with 200 W mercury arc (RUVF-203S, Radical Research Inc. (Hino, Japan)). The SO_3^\cdot radical was formed in $\text{KHCO}_3/\text{NaOH}$ buffer ($\text{pH} = 9.5$) from the photolysis of Na_2SO_3 [5, 8]. The hydroxyl and ethyl radicals were formed from the photolysis of hydrogen peroxide and triethyl lead acetate, respectively [9].

In order to determine spin trapping rates, we used a competitive trapping method, where two spin traps compete with each other to trap free radicals [3]. The sample solution was loaded in an ESR flat cell; ESR signals were immediately recorded with JEOL JES-FE3XG after UV irradiation: Sweep time 30 s, time constant 0.1 s, microwave power 3–5 mW, modulation amplitude 0.063 mT at 100 kHz. ESR spectra observed were computer-simulated with an attached computer program (WIN-RAD system, Radical Research Inc.) by superimposing the ESR spectra of two different radical adducts. The relative abundance of the adduct components was calculated with a computer-mediated double-integration routine of the first-derivative signal of each component.

The high-pressure ESR system used has been described elsewhere [10]. The sample solution was loaded into thick-walled quartz capillary tubing (ID 1 mm, OD 6 mm). After pressure was applied, the ESR signals of radical adducts generated with UV irradiation were recorded with an ESR spectrometer.

3 Results and discussion

3.1 Determination of spin trapping rates

Competitive spin trapping between two distinctive spin traps was used to determine the rate constants for the SO_3^\cdot and CO_2^\cdot trapping [3]. Figure 2 shows the typical ESR spectra obtained in the UV-irradiated solution of NaHCO_3 and H_2O_2 in the presence of two traps: (a) the PBN-DMPO and (b) CYPMPO-DMPO systems. Two spin adducts species are visible in these spectra; the hyperfine coupling constant (hfcc) values of spin adducts are listed in Table 1. The hfcc of the ESR spectra was assigned to the CO_2^\cdot radical adduct [7]. The ESR spectra of two different spin adducts were computer-simulated with an attached system (Figure 2a and b). The ESR spectra can be reproduced well by superimposing two components. The relative abundance of the adduct components was calculated using the simulation spectra.

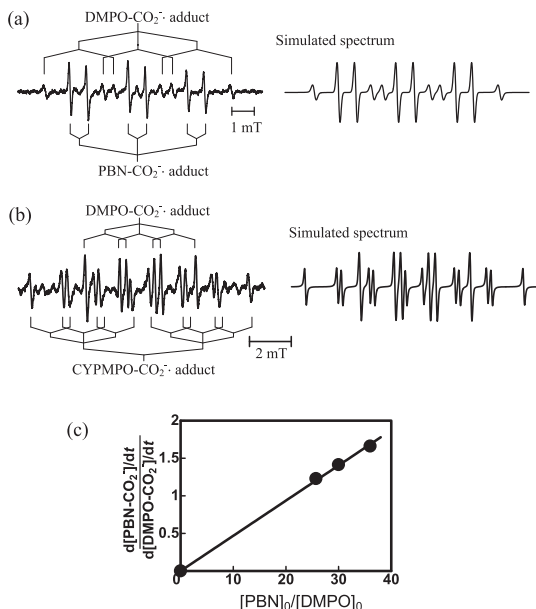
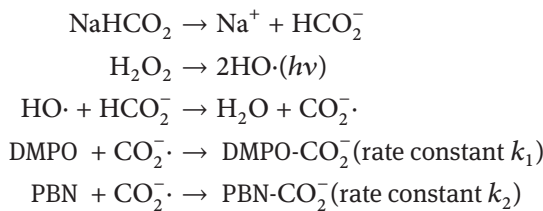


Figure 2: ESR spectra of carbon dioxide anion radical adducts obtained after UV-irradiation in (a) the PBN/DMPO and (b) CYPMPPO/DMPO systems at 298 K, and simulated spectra: (a) $[PBN]_0/[DMPO]_0 = 36$ and (b) $[CYPMPPO]_0/[DMPO]_0 = 0.19$. (c) Determination of k_{PBN}/k_{DMPO} according to Eq. (1) in the PBN/DMPO system.

The reaction scheme for spin trapping of CO₂[·] radical in the presence of PBN and DMPO is given by [7]:



The relative formation rates for DMPO-CO₂[·] and PBN-CO₂[·] adducts can be given as follows [10].

$$\frac{d[PBN-\text{CO}_2^{\cdot}]/dt}{d[\text{DMPO}-\text{CO}_2^{\cdot}]/dt} = \frac{k_2}{k_1} \frac{[PBN]_0}{[\text{DMPO}]_0} \quad (1)$$

where the symbol $[]_0$ denotes the initial concentration of traps. A typical plot of the concentration ratio of spin adducts against the initial concentration ratio of spin traps is shown in Figure 2c with a straight line passing through the origin, suggesting that the calculation process of relative trapping rate constants (k_2/k_1)

Table 1: Hyperfine coupling constants (hfcc) and rate constants for CO_2^\cdot and SO_3^\cdot at 298 K.

Spin Trap	Radical	hfcc (mT)			$k_2/k_1(\text{DMPO})$	$10^{-7} k_2$ ($\text{dm}^3 \text{mol}^{-1} \text{s}^{-1}$)
		A_{H}	A_{N}	A_{P}		
CYPMPO	CO_2^\cdot	1.666	1.461	5.343	7.70 ± 0.2	50.8
DPPMPO	CO_2^\cdot	1.790	1.398	3.931	4.31 ± 0.06	28.4
DEPMPO	CO_2^\cdot	1.735	1.448	5.167	5.44 ± 0.2	35.9
DMPO	CO_2^\cdot	1.871	1.572		1	6.6 ^{a)}
TMPO	CO_2^\cdot	1.981	1.581		$0.204 \pm 0.002^{\text{b)}$	1.48
2-Ph-DMPO	CO_2^\cdot		1.528		0.355 ± 0.003	2.34
4-POBN	CO_2^\cdot	0.348	1.550		1.76 ± 0.01	11.6
4-NO ₂ -PBN	CO_2^\cdot	0.414	1.576		1.30 ± 0.01	8.58
2-SO ₃ -PBN	CO_2^\cdot	0.620	1.580		0.0493 ± 0.0002	0.325
PBN	CO_2^\cdot	0.470	1.590		0.0458 ± 0.0006	0.302
4-HO-PBN	CO_2^\cdot	0.486	1.599		0.0272 ± 0.0002	0.18
CYPMPO ^{c)}	SO_3^\cdot	1.499	1.328	5.100	2.01 ± 0.06	2.41
		1.640 ^{d)}	1.550 ^{d)}	3.080 ^{d)}		
DPPMPO ^{c)}	SO_3^\cdot	1.497	1.294	3.812	1.21 ± 0.01	1.45
DEPMPO ^{c)}	SO_3^\cdot	1.521	1.358	5.002	1.46 ± 0.02	1.75
DMPO	SO_3^\cdot	1.615	1.453		1	1.2 ^{a)}
TMPO	SO_3^\cdot	1.300	1.410		$0.55 \pm 0.02^{\text{b)}$	0.064
4-POBN	SO_3^\cdot	0.160	1.480		0.034 ± 0.003	0.041
2-SO ₃ -PBN	SO_3^\cdot	0.459	1.586		0.0036 ± 0.0002	0.0043
PBN ^{c)}	SO_3^\cdot	0.197	1.498		0.0295 ± 0.0010	0.0354

^{a)} Cited from ref. [12].^{b)} The relative rate constants in the PBN/TMPO system.^{c)} Cited from ref. [6].^{d)} Diastereomeric spin adduct of CYPMPO against SO_3^\cdot .

using Equation (1) is justifiable. We determined the relative trapping rate constants of the SO_3^\cdot and CO_2^\cdot radicals for various PBN- and DMPO-type spin traps (Table 1). Further, in two new DMPO-type traps (CYPMPO and DPPMPO), the relative trapping rates for hydroxyl and ethyl radicals were determined according to Equation (1) (Table 2).

Determination of the reaction rate constants enables us to compare the trapping rates of various spin traps. In the present experiment, we determined the rate constants of SO_3^\cdot , CO_2^\cdot , $\text{C}_2\text{H}_5^\cdot$, and HO^\cdot for various traps by using previously published DMPO trapping rate constants. The rate constants of DMPO for SO_3^\cdot , CO_2^\cdot , $\text{C}_2\text{H}_5^\cdot$, and HO^\cdot were $k_{\text{DMPO}} = 1.2 \times 10^7$, 6.6×10^7 , 1.6×10^7 , and $3.6 \times 10^9 \text{ dm}^{-3} \text{ mol}^{-1} \text{ s}^{-1}$, respectively [11, 12]. The rate constants data for various traps are listed in Tables 1 and 2. The results show that, as a whole, the spin trapping rate constants of anionic radicals by DMPO-type traps are higher compared

Table 2: Hyperfine coupling constants (hfcc) and rate constants for $C_2H_5\cdot$ and $HO\cdot$ at 298 K.

Spin Trap	Radical	hfcc (mT)			k_2/k_1 (DMPO)	$10^{-7} k_2$ (dm ³ mol ⁻¹ s ⁻¹)
		A_H	A_N	A_P		
CYPMPO	$C_2H_5\cdot$	2.120	1.487	5.135	13.3 ± 0.1	21.3
DPPMPO	$C_2H_5\cdot$	2.273	1.487	3.635	2.74 ± 0.02	4.38
DMPO	$C_2H_5\cdot$	2.370	1.640		1	1.6 ^{a)}
CYPMPO	$HO\cdot$	1.407	1.407	5.160	7.67 ± 0.02	2800
		1.263 ^{b)}	1.386 ^{b)}	4.970 ^{b)}		
DPPMPO	$HO\cdot$	1.370	1.370	3.550	2.36	850
DMPO	$HO\cdot$	1.530	1.530		1	360 ^{c)}

^{a)} Cited from ref. [12].^{b)} Diastereomeric spin adduct of CYPMPO against $HO\cdot$.^{c)} Cited from ref. [11].

with those of PBN-type traps. In particular, CYPMPO and DEPMPO are effective for scavenging the anionic $SO_3^{\cdot-}$ and $CO_2^{\cdot-}$ radicals.

3.2 Substituent effects on spin trapping

The Hammett plot may be useful for a discussion on substituent effects on the spin trapping reaction. However, substituent constants for various traps are not available. In a previous paper, we determined the $\cdot OH$ radical trapping rate constants for various traps [9]. The $\cdot OH$ radical is recognized as a non-selective oxidant and readily undergoes addition reaction to the phenyl groups or double bonds [13]. Thus, we believe that the $\cdot OH$ radical trapping rate constants reflect the reactivity of the traps, while the effects of the substituent are small. Using the trapping rate constants in Table 2 and the previously observed trapping data for $\cdot OH$ radical [9], alternatively, we plotted the spin trapping rate constants of $SO_3^{\cdot-}$ and $CO_2^{\cdot-}$ against those of $\cdot OH$, together with those of $C_2H_5\cdot$ (Figure 3). Figure 3a clearly suggests that PBN-type trapping rate constants for $CO_2^{\cdot-}$ tend to increase with an electron-withdrawing group in the traps (slope in Figure 3a = 2.4) compared with that of $C_2H_5\cdot$ (slope = 1.3). However, the trapping rate constants for $SO_3^{\cdot-}$ are independent of the substituents in the PBN traps (slope = 0.20), which is ascribed to the difference in the contribution to the resonance system in the PBN traps. In the DMPO type spin trapping, as shown in Figure 3b, the effects of substituent on the trapping rates of two anionic radicals are small compared with those of the $C_2H_5\cdot$ radical, which is responsible for the small electron-inductive effect of the

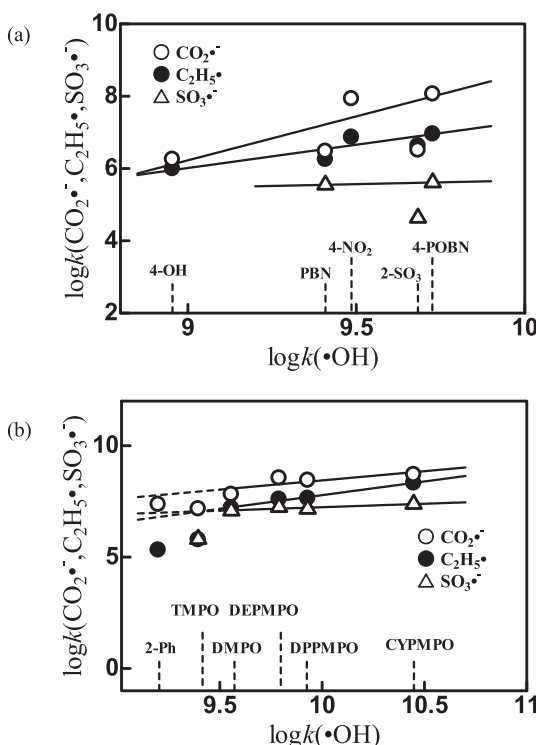


Figure 3: Relationship of trapping rate constants of CO_2^\cdot , SO_3^\cdot , and $\text{C}_2\text{H}_5^\cdot$ for those of $\text{HO}\cdot$: (a) PBN- and (b) DMPO-type traps. The available trapping data of $\text{C}_2\text{H}_5^\cdot$ and $\text{HO}\cdot$ were cited from ref. [9].

SO_3^- and CO_2^- groups: the slopes in Figure 3b were calculated to be 0.82 (CO_2^-), 0.31 (SO_3^-), and 1.2 ($\text{C}_2\text{H}_5^\cdot$).

2-Ph-DMPO and TMPO exhibit a downward shift in the trapping rates as compared with those of the DMPO-type traps in Figure 3b. These may be attributed to the steric hindrance caused by the phenyl- and methyl-substituent groups.

3.3 Pressure effects on spin trapping

Using the pressure dependence of the relative rate constants (Table 3), we evaluated the difference in the activation volumes ($\Delta\Delta V^\ddagger$) for the two trapping pro-

Table 3: External pressure dependence of relative trapping rate constants and activation volumes.

Traps	Radical				k_2/k_1	$\Delta\Delta V^\ddagger$
		1	98	245	490 (bar)	(cm ³ mol ⁻¹)
4-POBN/DMPO	CO ₂ ⁻ ·	1.76 ± 0.08	1.96	1.99	2.28	-13
4-POBN/DMPO	SO ₃ ⁻ ·	0.0340 ± 0.0010	0.0332	0.0327	0.0307	4.9
4-POBN/DMPO	C ₂ H ₅ ·	0.570 ± 0.05	0.580	0.620	0.682	-8.9
PBN/DMPO	CO ₂ ⁻ ·	0.0458 ± 0.0012	0.0483	0.05927	0.0788	-27
PBN/DMPO	SO ₃ ⁻ ·	0.0295 ± 0.0009	0.0316	0.0365	0.0434	-19
PBN/DMPO ^{a)}	C ₂ H ₅ ·	0.111 ± 0.014	0.112	0.115	0.118	-4.1
CYPMPO/DMPO	CO ₂ ⁻ ·	7.70 ± 0.15	7.79	8.83	10.1	-13
CYPMPO/DMPO	SO ₃ ⁻ ·	2.01 ± 0.09	2.14	2.24	2.55	-12
CYPMPO/DMPO	C ₂ H ₅ ·	13.3 ± 0.05	14.2	15.0	16.7	-12
DEPMPO/DMPO	CO ₂ ⁻ ·	5.44 ± 0.14	5.68	6.15	6.62	-10
DEPMPO/DMPO	SO ₃ ⁻ ·	1.46 ± 0.09	1.54	1.58	1.82	-10
DEPMPO/DMPO	C ₂ H ₅ ·	2.53 ± 0.08	2.68	2.84	3.07	-10
PBN/TMPO	CO ₂ ⁻ ·	0.204 ± 0.011	0.212	0.236	0.265	-13
PBN/TMPO	SO ₃ ⁻ ·	0.550 ± 0.08	0.576	0.594	0.621	-6.4
PBN/TMPO ^{a)}	C ₂ H ₅ ·	2.82 ± 0.05	2.74	2.63	2.49	6.5

^{a)} Cited from ref. [9].

cesses (ΔV_1^\ddagger and ΔV_2^\ddagger) according to the following equations:

$$\ln(k_2/k_1) = aP + b \quad (2)$$

$$\Delta\Delta V^\ddagger = -RT(\partial \ln(k_2/k_1)/\partial P)_T = \Delta V_2^\ddagger - \Delta V_1^\ddagger \quad (3)$$

The slope of the best-fit straight line in a plot for $\ln(k_2/k_1)$ against pressure was used to estimate $\Delta\Delta V^\ddagger$ for two trapping processes (Figure 4) and the results are listed in Table 3. An inspection of Table 3 suggests that the $\Delta\Delta V^\ddagger$ values ($= -27$ – 4.9 cm³ mol⁻¹) for PBN and 4-POBN against DMPO are dependent on the kinds of trapped radicals, while those ($= -13$ – -10 cm³ mol⁻¹) of CYPMPO and DEPMPO against DMPO are independent of the trapped radicals. In a previous paper, Sueishi et al. suggested that PBN-type traps have the steric crowded trapping site as compared with those of DMPO, resulting in the negative $\Delta\Delta V^\ddagger$ values for the PBN/DMPO system.

It is instructive to examine the trapping reactions of the 4-POBN/PBN and TMPO/DMPO systems for the discussion on reaction mechanisms. In radical trapping by the PBN- and DMPO-type traps, we can calculate the difference in activation volumes for the various trapping processes by using the $\Delta\Delta V^\ddagger$ values in

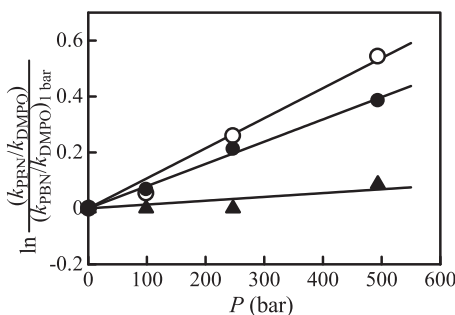


Figure 4: Plots of relative trapping rate constants against external pressures in the PBN/DMPO system: (○) CO_2^{\cdot} , (●) SO_3^{\cdot} , and (▲) $\text{C}_2\text{H}_5^{\cdot}$ radical trapping. The available trapping data of $\text{C}_2\text{H}_5^{\cdot}$ were cited from ref. [9].

Table 3:

$$\Delta\Delta V_{4-\text{POBN}/\text{PBN}}^{\ddagger} = \Delta V_{4-\text{POBN}}^{\ddagger} - \Delta V_{\text{PBN}}^{\ddagger} = \Delta\Delta V_{4-\text{POBN}/\text{DMPO}}^{\ddagger} - \Delta\Delta V_{\text{PBN}/\text{DMPO}}^{\ddagger} \quad (4)$$

$$\Delta\Delta V_{\text{TMPO}/\text{DMPO}}^{\ddagger} = \Delta V_{\text{TMPO}}^{\ddagger} - \Delta V_{\text{DMPO}}^{\ddagger} = \Delta\Delta V_{\text{PBN}/\text{DMPO}}^{\ddagger} - \Delta\Delta V_{\text{PBN}/\text{TMPO}}^{\ddagger} \quad (5)$$

The $\Delta\Delta V_{4-\text{POBN}/\text{PBN}}^{\ddagger}$ and $\Delta\Delta V_{\text{TMPO}/\text{DMPO}}^{\ddagger}$ values ($\text{cm}^3 \text{mol}^{-1}$) were calculated to be 14 (CO_2^{\cdot}), 24 (SO_3^{\cdot}), and -4.8 ($\text{C}_2\text{H}_5^{\cdot}$) for the 4-POBN/PBN system and -13 (CO_2^{\cdot}), -13 (SO_3^{\cdot}), and -11 ($\text{C}_2\text{H}_5^{\cdot}$) for the TMPO/DMPO system. The negative value for $\text{C}_2\text{H}_5^{\cdot}$ -trapping in the 4-POBN/PBN system can be explained in terms of the localization of the π -electrons upon trapping with 4-POBN [9]. The large positive values for anionic radicals trapping in 4-POBN/PBN is ascribed to desolvation for the less polar activation complex of ionic radicals upon trapping by 4-POBN having the electron-withdrawing group. Negative $\Delta\Delta V^{\ddagger}$ values (ca. $-10 \text{ cm}^3 \text{ mol}^{-1}$) for the substituted-DMPO/DMPO system (DEPMPO and CYPMPO) indicate that the degree of steric crowding in the transition state for DEPMPO and CYPMPO spin trapping is higher than that in DMPO spin trapping. In the spin trapping of the TMPO/DMPO system, the negative $\Delta\Delta V^{\ddagger}$ value for radical trapping can be explained in terms of the steric hindrance around the TMPO trapping site [9, 14], suggesting that the steric hindrance in the DEPMPO and CYPMPO traps having bulky substituent groups is comparable to that by methyl groups around the TMPO trapping site. Using the $\Delta\Delta V^{\ddagger}$ values for the DMPO-trapping reaction of $\text{C}_2\text{H}_5^{\cdot}$ and CO_2^{\cdot} (Table 3), the volume profile for the trapping reactions is shown in Figure 5. It is noted that PBN-type traps show the characteristic effect of external pressure, depending on the nature of the trapped radicals.

In conclusion, the spin trapping rate constants of various substituted-PBN and -DMPO traps for hydroxyl, ethyl, and anionic radicals (CO_2^{\cdot} and SO_3^{\cdot}) were

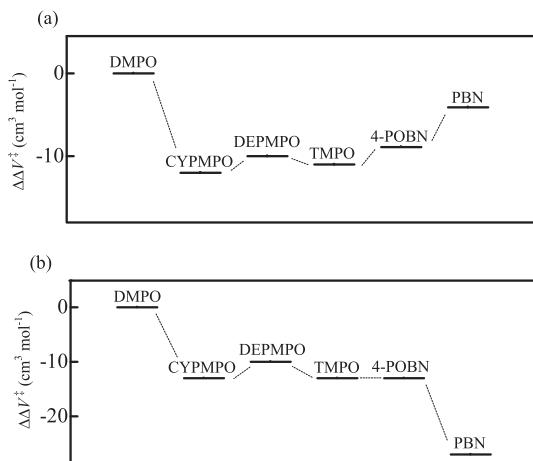


Figure 5: Volume profile ($\Delta\Delta V^\ddagger$) of the trapping reactions with various traps for DMPO-trapping: (a) $\text{C}_2\text{H}_5\cdot$ and (b) $\text{CO}_2\cdot^-$.

determined using a competitive ESR trapping method. The influences of substituent and external pressure on the spin trapping rates of various traps for anionic radicals were shown. A steric crowded trapping site of DMPO-type traps such as CYPMPO and DEPMPO is responsible for the pressure-induced acceleration in trapping rates (the negative ΔV^\ddagger values). High-pressure studies provided useful insight into the spin trapping reaction mechanism.

Acknowledgement: We thank Dr. Yashige Kotake for helpful discussion of the manuscript.

References

1. E. G. Janzen, Accounts Chem. Res. **4** (1971) 31.
2. G. R. Buettner, Free Radical Bio. Med. **3** (1987) 259.
3. Y. Sueishi, C. Yoshioka, C. Claudio-Azar, L. A. Reinke, and Y. Kotake, B. Chem. Soc. Jpn. **75** (2002) 2043.
4. H. D. Rabinowitch, G. M. Rosen, and I. Fridovich, Free Radical Bio. Med. **6** (1989) 45.
5. C. Mottley and R. P. Mason, Arch. Biochem. Biophys. **267** (1985) 681.
6. Y. Sueishi, A. Miyata, D. Yoshioka, M. Kamabayashi, and Y. Kotake, J. Incl. Phenom. Macro. **66** (2010) 357.
7. F. A. Villamena, E. J. Locigno, A. Rockenbauer, C. M. Hadad, and J. L. Zweier, J. Phys. Chem. A **110** (2006) 13253.

8. C. Mottley, R. P. Mason, C. F. Chignell, K. Sivarajah, and T. E. Eling, *J. Biol. Chem.* **257** (1982) 5050.
9. Y. Sueishi, D. Yoshioka, C. Yoshioka, S. Yamamoto, and Y. Kotake, *Org. Biomol. Chem.* **4** (2006) 896.
10. Y. Sueishi, S. Yamamoto, and N. Nishimura, *Meas. Sci. Technol.* **4** (1993) 1171.
11. R. Sridhar, P. C. Beaumont, and E. L. Powers, *J. Radioanal. Nucl. Ch.* **101** (1986), 227.
12. H. Taniguchi and K. P. Madden, *J. Am. Chem. Soc.* **121** (1999) 11875.
13. K. Hata, M. Lin, Y. Katsumura, Y. Muroya, H. Fu, S. Yamashita, and H. Nakagawa, *J. Radiat. Res.* **52** (2011) 15.
14. M. G. Gonikberg, *High Pressure Chemistry*, Nikkan Kogyo Shinbun, Tokyo, 1972.